TEXTURING TECHNIQUES AND RESULTING SOLAR CELL PARAMETERS ON TRI-SILICON MATERIAL

D. Sontag[1], G. Hahn[1], P. Fath[1], E. Bucher[1] and W. Krühler[2]
1. University of Konstanz, Faculty of Physics, 78457 Konstanz, Germany
2. Shell Solar, Otto-Hahn-Ring 6, 81739 Munich, Germany

ABSTRACT

Tri-crystalline silicon material (Tri-Si) is a promising alternative to mono-crystalline CZ silicon because of a faster crystallization process and higher wafer stability. The orientation of the three crystals (110) is different to the (100) orientation in CZ material typically used in the photovoltaic industry. As a consequence the common alkaline texture technique using KOH or NaOH cannot be applied. For this reason we compared several alternative texturing methods like mechanical grooving and acidic texture etching, which work independently of crystal orientations. Solar cells were processed from these wafers, and an overview of their surface morphology as well as the resulting cell parameters is given. By applying an antireflection coating we reached the highest efficiencies reported on Tri-Si material.

1. INTRODUCTION

There are different techniques to texture the surface of solar cells, but as Tri-Si has a deviating crystal orientation as compared to CZ material [1], alkaline texturing methods commonly used for industrial processes are not applicable. Experiments with an acidic texture on Tri-Si were published recently, resulting in efficiencies of 17.6% [2]. In this paper two different texturing techniques are examined. On the one hand we textured wafers with a dicing saw, ending up with V-grooves in the surface, while on the other hand an acidic etching solution developed at Shell-Solar in Munich was used.

2. TEXTURING

2.1 V-groove texture

The first method we used for reducing the reflectivity of Tri-Si wafers is the mechanical V-texture technique as described in [3]. The structuring can be performed with a dicing saw either by using a single blade or a multi-blade roll. In certain distances plateaus have to remain, where at the end of the process the front grid will contact the emitter. In Figure 1 such a plateau is visible with a finger on top of it. Problems can occur if the photolithographically defined metallisation runs perpendicularly to the grooves. In this case line discontinuities can appear as shown in Figure 1. Here the finger connection line on the opposite side of the busbar is disconnected by the grooves. The reflectivity decreases with smaller angles of the grooves, but the smaller the angles, the lower is the stability and the higher is the increase of the surface area. Simulations have been carried out to find the optimal angle for lowest reflectivity [3]. According to the results we used a blade which results in 35° angles of the grooves and a groove depth of 70 µm.

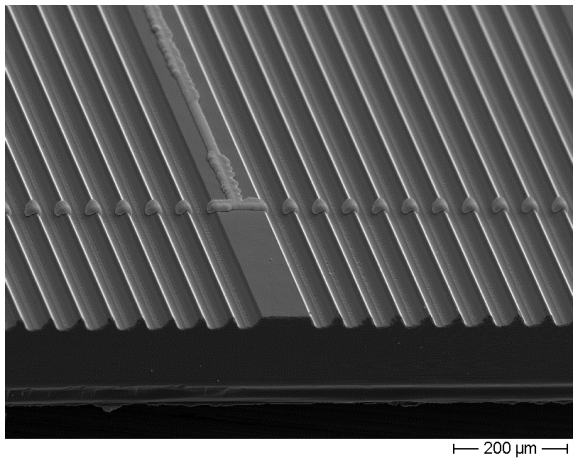

Fig. 1 Mechanically V-grooved surface of a Tri-Si wafer. A plateau is visible with an electro-plated front grid and the dotted finger connection line, which is supposed to be solid.

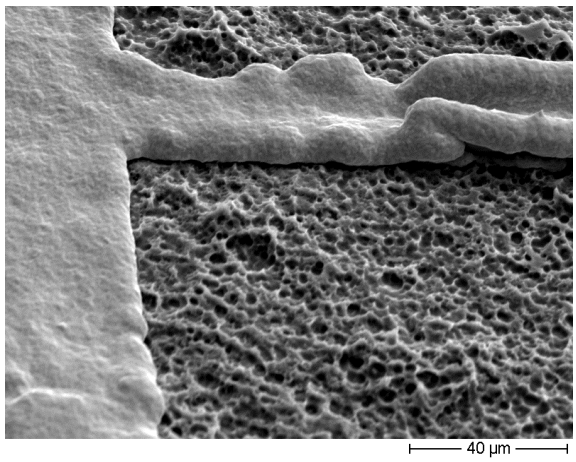

Fig. 2 Electron microscopic picture of an acidic textured Tri-Si wafer after electro-plating. On the left hand side the busbar is visible, connected to a finger.

To counteract any photolithographical problems, the grooves end right before the busbar. As the blade is not perfectly sharp, the grooves are rounded at the bottom. The surface increase of an optimal textured wafer would be around 150%, in this experiment however the saw

damage etching was too long, so we ended up with a surface increase of only around 45%.

2.2 Acidic texture

The second technique for texturing Tri-Si wafers used in this experiment is an acidic texture developed at Shell-Solar in Munich. It consists of sulfuric acid, hydrofluoric acid and nitric acid in the ratio 6:3:1, and is used at room temperature. By applying this texture we end up with a porous layer on top of the surface, which can be easily removed by a dip in an aqueous solution of NaOH (10%). An electron microscopic picture of the surface is presented in Figure 2. The porous layer is etched off and the electro-plated busbar as well as one finger can be seen on the picture. By the sponge like structure, the surface is increased by approximately 50%, assuming that the holes are hemispheres and equally spread over the whole surface. Problems can occur if the porous layer has not been removed completely. In this case it prevents the surface below from being passivated by an oxide or nitride, resulting in a higher surface recombination.

3. EXPERIMENT

3.1 Cell fabrication

For our experiments we used Tri-Si material with a bulk resistance of 4-6 Ωcm. Due to the high content of oxygen ($0.8\text{-}1.2\cdot10^{18}$ cm^{-3}), this material is sensitive to temperatures in the range between 600°C and 800°C. Within this interval new donors are formed [4]. They are electrically active and can reduce the diffusion lengths of minority charge carriers. For this reason all high temperature steps were carried out using fast up and down ramps.

The whole process sequence is illustrated in Figure 3. First of all the saw damage has to be removed. As the wafers for our experiment have been cut with an ID-saw, resulting in a deep surface damage, we removed about 60 µm from each side. The next step is to texture the surface. The mechanical texture is applied only at the front surface and has to be etched to remove the saw damage of the grooving, while the acidic solution textures front- and back surface.

The emitter is formed by a $POCl_3$-diffusion. We chose a sheet resistance of 100 Ω/sq. This process step produces a P-glas layer, which has to be removed by a HF-dip. After that the front surface is covered by an oxide to reduce the recombination of the charge carriers in that region. As this layer changes the refractive index of the surface the anti reflection coating (ARC) used in this experiment (see. Chap. 4) is no longer optimal. To minimize this effect we chose a thin oxide of around 10 nm, which passivates the surface sufficiently but has no major influence on the reflectivity after ARC.

The back contact is applied by aluminum screen printing followed by a firing step in a belt furnace as normally used in industrial processes. As Tri-Si material has high minority carrier diffusion lengths (up to 1000 µm [5]) it is important to have a good back side passivation. Screen-printing is an easy and fast method to form the back contact in combination with a good back surface field (BSF), which reflects incoming charge carriers back into the bulk and prevents them from recombining at the back surface. The BSF produced with this method reduces the recombination velocity from 10^5-10^6 cm/s without BSF to 200 cm/s.

The front grid consists of Ti/Pd/Ag, evaporated onto the emitter after a photolithographic masking. To reduce the series resistance in the fingers, the metallisation is thickened by electro-plating. The following sintering step reduces the contact resistance. Finally the edges are isolated by dicing 2x2 cm² solar cells out of the processed 5x5 cm² wafers.

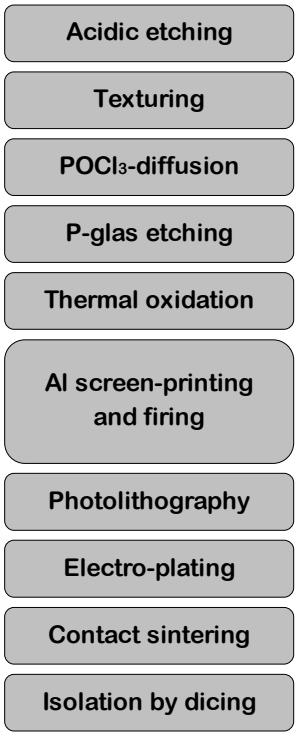

Fig. 3 Processing sequence used in this study. In order to achieve a low back surface recombination we used a screen printed Al-BSF. The front grid has been evaporated after photolithographic masking.

3.2 Characterization

In the following examination only the data of the best solar cell of each type of surface texture is used. One of the major interests when examining different textures is the resulting reflectivity of the wafers. The reflectivities of solar cells with different textures and without any ARC are plotted in Figure 4. A significant reduction in reflectivity after texturing can be observed. The mean weighted values between 300 nm and 1200 nm decrease from 36% for the untextured solar cell to 25% for the textured solar cells (the acidic textured as well as the V-textured). Unfortunately the V-texture in this experiment was not optimal, because the extended saw damage etching step after mechanical texturing (see chap. 2.1) resulted in rounded grooves correlated to a higher reflectivity. To give an impression of the potential of this texturing technique the reflectivity of an optimal V-textured solar cell is additionally plotted in Figure 4. Its mean remaining reflectivity is about 15%.

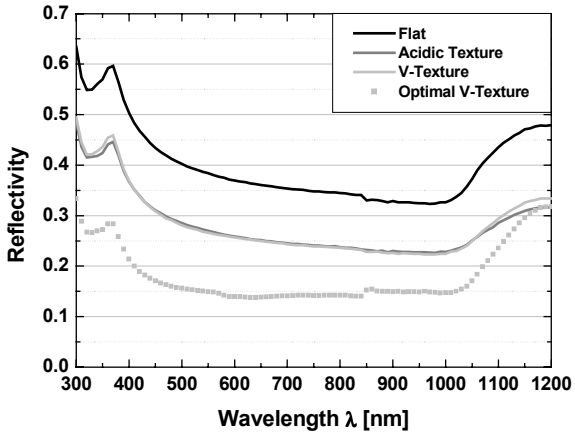

Fig. 4 Reflectivities of solar cells with different surface textures without any ARC. Additionally the reflectivity curve of an ideal V-textured solar cell is plotted to visualize the potential of this texturing technique.

4. SOLAR CELL RESULTS

The internal quantum efficiencies (IQE) of the three solar cells are displayed in Figure 5. There is a slight increase in the long wavelength region for textured cells, especially for the V-textured cell. This correlates with the fact, that by entering the cell through a rough surface, a perpendicular incoming photon is scattered, so its way through the wafer is longer and the probability for charge carrier generation is higher.

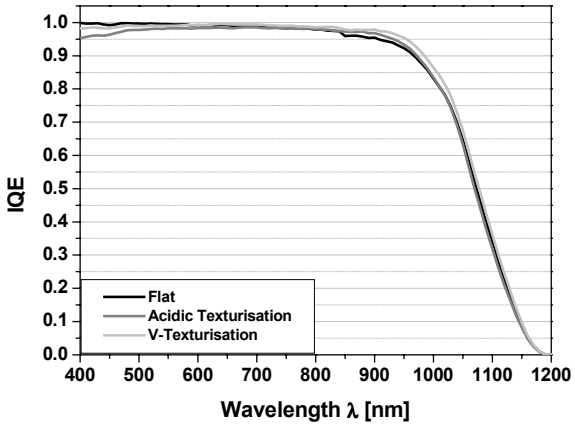

Fig. 5 Internal quantum efficiencies of the three Tri-Si solar cells with different surface morphology. Textured cells tend to higher values in the long wavelength region, but they also show a loss for short wavelengths.

However, short wavelength photons enter the wafer only a few microns, so the influence of the space charge region (SCR) and the surface increase. Only if the surface is very well passivated its increase by texturing is of minor importance for recombination. But the area of the SCR also increases for textured cells and so does the recombination in the SCR. The consequence is a rising J_{02} (see Table I), resulting in a lower fill factor (see Table II) and also slightly lower IQE values in the region of short wavelengths. After these measurements the front surfaces were covered by a double layer ARC (ZnS/MgF_2) resulting in significantly lower reflectivities (see Figure 6). The values of the textured cells are approximately $30\%_{rel}$ lower than the values of the untextured one.

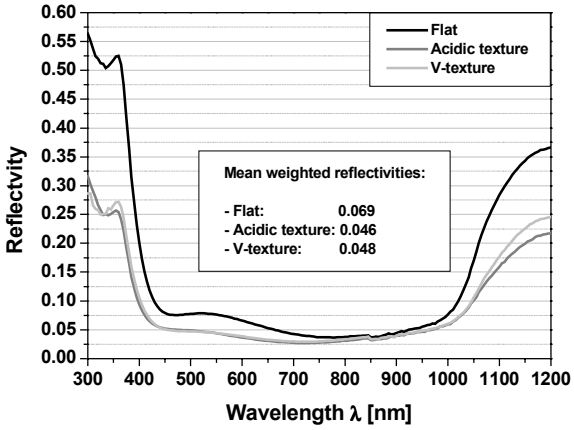

Fig. 6 Reflectivities of the tree solar cells with a DARC. The mean weighted values of the textured cells are approximately $30\%_{rel}$ lower than the values of the untextured cell.

The dark IV curves of the tree solar cells are displayed in Figure 7 and the extracted values are shown in Table I. Clearly visible are the decreased shunt resistances for the textured cells. Corresponding to the surface increases described in chapter 2, we find a significant increase of J_{02} for the V-textured as well as for the acidic textured cell.

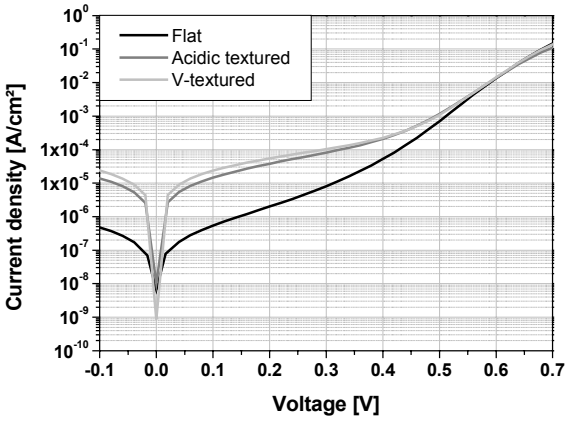

Fig. 7 Dark IV curves of the three solar cells with DARC. Decreased shunts for textured solar cells.

Table I. Parameters of all three solar cells, extracted from dark IV data. J_{02} increases with surface enlargement of the SCR while the shunt resistance R_{sh} decreases.

Surface	R_{sh} [Ωcm²]	R_s [Ωcm²]	J_{01} [A/cm²]	J_{02} [A/cm²]
Flat	$1.8 \cdot 10^5$	0.24	$9.3 \cdot 10^{-13}$	$1.8 \cdot 10^{-8}$
Acidic Texture	$6.4 \cdot 10^3$	0.24	$4.7 \cdot 10^{-13}$	$6.3 \cdot 10^{-8}$
V-Texture	$3.8 \cdot 10^3$	0.23	$6.4 \cdot 10^{-13}$	$5.9 \cdot 10^{-8}$

Resulting parameters from illuminated IV measurements are shown in Table II. As expected, there is a significant increase in J_{SC} for the textured solar cells and

according to this also in efficiencies. However the fill factors dropped by $1\%_{abs}$, because of the enlarged SCR and the correlated J_{02} increase. Parameters of the V-textured cell are independently confirmed by EC JRC Ispra (see Table II, gray values). This solar cell has the highest efficiency reported on Tri-Si.

Table II. Cell parameters of the three differently textured solar cells. The independently confirmed parameters by EC JRC Ispra for the V-textured solar cell are indicated in gray.

Surface	J_{SC} [mA/cm²]	V_{OC} [mV]	FF [%]	η [%]
Flat	37.3	632	78.7	18.5
Acidic Texture	37.8	629	77.7	18.5
V-Texture	38.2	629	77.7	18.7
	38.6	**625**	**77.8**	**18.8**

All of the cells include at least one grain boundary (see Fig. 8). The purpose of this sketch is to clarify the position of the solar cells within a Tri-Si wafer. The solar cells themselves originate all from different wafers.

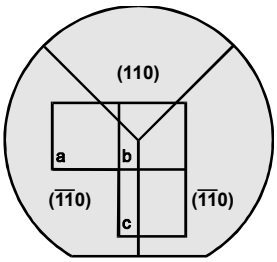

Fig. 8 Positions of the solar cells on a four inch Tri-Si wafer. They all include at least one grain boundary.
a) Acidic textured
b) Flat
c) V-textured

The triple point is included in the untextured solar cell. To check if twin boundaries in Tri-Si are harmful for the cell parameters, we performed spatially resolved LBIC and reflectivity measurements of the flat cell and calculated the IQE (see Fig. 9). The grain boundaries are visible and reducing the IQE, with the vertical second-order twin boundary seeming to be less electrically active than the first-order ones, but regarding the scaling of the map this decrease is rather marginal. Even the region around the triple point with the lowest values still reveals an IQE of 0.85 (2.7% deviation to peak value) corresponding to an effective diffusion length of more than 450 µm. Considering a cell thickness of 200 µm this is still sufficient for most of the charge carrier to reach the SCR and to contribute to the electrical current.

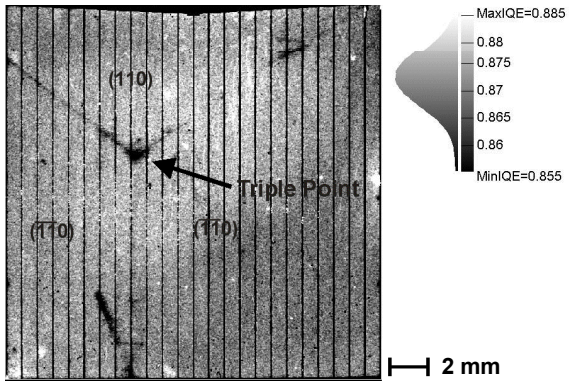

Fig. 9 IQE at 980 nm of the untextured solar cell. The twin grain boundaries are visible, but regarding the scaling of the histogram they are only slightly electrically active.

5. CONCLUSION

Both texturing techniques, mechanical V-grooving as well as acidic texturing, can be used for texturing Tri-Si wafers in order to increase efficiencies. While the V-groove technique has the potential for very low reflectivities, the acidic texturing is faster and easier to handle.

Solar cells have been manufactured, resulting in short circuit currents above 38 mA/cm². A gain of 2.5% in J_{SC} as compared to the untextured reference could be obtained. Although the fill factor decreased by $1\%_{abs}$, we end up with efficiencies of up to 18.8% after deposition of a DARC. This is the highest efficiency reported for Tri-Si. By optimizing the V-texture it should be possible to achieve a further reduction in reflectivity and an additional increase in efficiency.

6. ACKNOWLEDGEMENTS

This work was supported within the KoSi program by the German Bundesministerium für Wirtschaft (BMWi) under contract number 0329858J.

7. REFERENCES

[1] D. Cavalcoli, A. Cavallini, C. Capperdoni, D. Palmeri, G. Martinelli; Semicond. Sci. Technol. **10** (1995) 660-665

[2] C. Schmiga, J. Schmidt, A. Metz, A. Endrös, R. Hetzel; Prog. Photovolt: Res. Appl. 2003; **11**:33-38

[3] C. Gerhards, F. Huster, M. Spiegel, C. Marckmann, P. Fath, E. Bucher; 2nd WCEPSEC (1998) Vienna

[4] D. Karg, A. Voigt, G. Pensl, M. Schulz, H.P. Strunk, W. Zulehner, Phys. Stat. Sol. (b), **210,** 533 (1998)

[5] A. L. Endrös; Sol. En. Mat. & Sol. Cells 72 (2002) 109-124